Bioorganic & Medicinal Chemistry 20 (2012) 3058–3064

Contents lists available at SciVerse ScienceDirect

Bioorganic & Medicinal Chemistry

journal homepage: www.elsevier.com/locate/bmc

Oxovanadium complexes with quinoline and pyridinone ligands: Syntheses of the complexes and effect of alkyl chains on their apoptosis-inducing activity in leukemia cells

Tomoko Yamaguchi [a], Shinya Watanabe [b], Yuriko Matsumura [a], Yoshikazu Tokuoka [b], Akihiro Yokoyama [a,*]

[a] Department of Materials and Life Science, Faculty of Science and Technology, Seikei University, 3-3-1 Kichijoji-kitamachi, Musashino, Tokyo 180-8633, Japan
[b] Department of Medical Technology, Faculty of Biomedical Engineering, Toin University of Yokohama, 1614 Kurogane-cho, Aoba-ku, Yokohama 225-8503, Japan

ARTICLE INFO

Article history:
Received 25 December 2011
Revised 24 February 2012
Accepted 25 February 2012
Available online 14 March 2012

Keywords:
Vanadium
Apoptosis
Quinoline
Pyridinone
Caspase

ABSTRACT

Vanadium complexes with quinoline ligands (**1b**–**g**) and pyridinone ligands (**2b**–**d**) were synthesized, and the effect of the length and shape of alkyl chains on the antiproliferative activity toward U937 cells was studied. For the synthesis of the vanadium complexes, quinoline and pyridinone ligands were prepared and then treated with $VOSO_4$ or $VO(acac)_2$. The vanadyl(IV) complexes were characterized by IR, ESR, and UV–vis spectroscopy and elemental analyses. The antiproliferative activity of **1a**–**g** toward U937 cells showed little dependence on the length and shape of the alkyl chain. In contrast, a good correlation was found between the IC_{50} values and partition coefficients (log*P*) values of **2a**–**c**. Among them, **2c** showed the highest inhibitory activity, and its IC_{50} value was smaller than that of cisplatin. The apoptosis-inducing ability of **2b** and **2c** was supported by annexin V-propidium iodide staining experiments and agarose gel electrophoresis analysis. Inhibitors of caspase-3, -8, and -9 did not affect the antiproliferative activity of **2c**, indicating that the apoptosis induced by **2c** was via a caspase-independent pathway.

1. Introduction

Various metal complexes have been investigated and used as anticancer agents.[1] For example, platinum-containing complexes such as cisplatin (*cis*-diammineplatinum(II) dichloride) and carboplatin are some of the most potent, widely used chemotherapeutic drugs.[2] However, these compounds cause strong side effects, which limit their use. Several vanadium complexes also show antitumor activities.[3,4] Among them, oxovanadium complexes with maltol and phenanthroline ligands have been reported to induce apoptosis in various cancer cell lines.[5–9] Recently, compounds that induce apoptosis in cancer cells have attracted much attention because they may provide a novel approach to cancer therapy.[10,11]

The anticancer activities of the metal complexes are largely affected by their lipophilicity because the complexes have to cross the hydrophobic cell membranes to exhibit their activity. For example, the dinuclear Ru-arene complex with 12 CH_2 linking chains shows higher cytotoxicity in the cancer cell lines A2780 and SW480 than complexes with three or six CH_2 chains.[12] The lipophilicity of non-metallic compounds, such as bis-galloyl derivatives[13] and alkenyl and alkyl trisulfide,[14] is also important for their antiproliferative activities.

We have studied the bioactivities of vanadium complexes, and reported that oxovanadium(IV) complexes with the dipentylsulfamoylquinoline unit (**1a**) and *N*-butylpyridinone unit (**2a**) showed greater antiproliferative activity against leukemia cells than the complexes with the dimethylsulfamoylquinoline unit and *N*-methylpyridinone unit, respectively.[15] We expected that if we could optimize the lipophilicity by changing the length of the alkyl chain of the ligand, the activity of the complexes would increase because of improved membrane permeability. In the present study, we report the synthesis of the vanadyl complexes **1** and **2** with quinoline and pyridinone ligands having different alkyl chains (Fig. 1). We also report the effects of the lipophilicity of the complex on its apoptosis-inducing activity in U937 cells. When the ligand of the vanadium complex was a quinoline derivative, a clear relationship was not observed between the length of the alkyl chain and activity. However, the activity of the complex with pyridinone ligands increased with the length of the alkyl chain. In addition, the mechanism of the cytotoxicity induced by the vanadyl complexes was investigated.

2. Experimental

2.1. General

IR spectra were recorded using a JASCO FT/IR-470 system. ^1H NMR spectra were obtained on a JEOL JNM-LA400D NMR

* Corresponding author. Tel.: +81 422 37 3463; fax: +81 422 37 3871.
E-mail address: ayokoyama@st.seikei.ac.jp (A. Yokoyama), ayokoyama@st.seikei.ac.jp (A. Yokoyama).

0968-0896/$ - see front matter © 2012 Elsevier Ltd. All rights reserved.
http://dx.doi.org/10.1016/j.bmc.2012.02.063

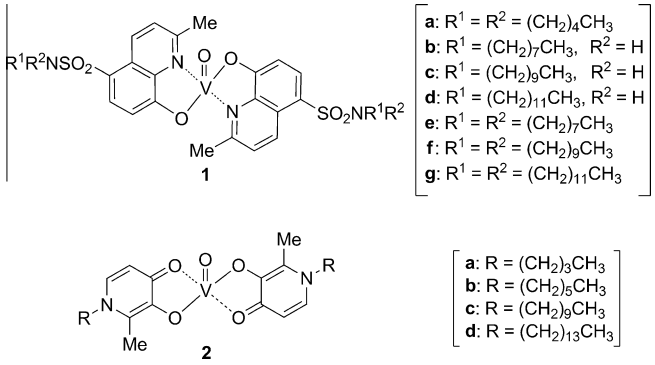

Figure 1. Structure of vanadium complexes **1a**–**g** and **2a**–**d**.

spectrometer. Tetramethylsilane was used as an internal reference. Thin-layer chromatography and column chromatography were conducted on Merck Silica Gel 60 F_{254} and Merck Silica Gel 60 (70–230 mesh), respectively. Elemental analysis was carried out using a Perkin–Elmer 2400 analyzer series II or a Euro Vector EUROEA3000-Dual system. All chemicals were of reagent grade and used without further purification. ESR spectra were obtained on a JEOL TE-300 X-band ESR spectrometer. The complexes **1b**–**g** and **2b**–**d** were dissolved in tetrahydrofuran (THF), and the solution was transferred to a glass capillary tube for ESR measurement. The typical measuring conditions are following: microwave power, 1.0 mW; modulation frequency, 100 kHz; modulation amplitude width, 2.0 mT; response, 0.3 s; scanning time, 4 min; magnetic field, 325 ± 75 mT; temperature, room temperature. The isotropic hyperfine coupling constants (*A* values) and *g* value were obtained from the spectra. Stained cells were observed with a Nikon ECLIPS ETE300 fluorescence microscope. An Annexin V-Fluorescein Staining Kit was obtained from Wako Pure Chemical Industries Ltd. Electrophoresis was performed with an ADVANCE Mupid-Scope. *N*-Benzyloxycarbonyl-Asp(OCH_3)-Glu(OCH_3)-Val-Asp(OCH_3)-fluoromethyl ketone (Z-DEVD-FMK, caspase-3 inhibitor), *N*-benzyloxycarbonyl-Ile-Glu-Thr-Asp-fluoromethyl ketone (Z-IETD-FMK, caspase-8 inhibitor), *N*-benzyloxycarbonyl-Leu-Glu(OCH_3)-His-Asp(OCH_3)-fluoromethyl ketone (Z-LEHD-FMK, caspase-9 inhibitor), and *N*-benzyloxycarbonyl-Val-Ala-Asp-fluoromethyl ketone (Z-VAD-FMK, general caspase inhibitor) were purchased from Medical & Biological Laboratories Co., Ltd. The octanol/water partition coefficients of the vanadium complexes were estimated as reported previously.[16] HPLC analyses were undertaken using a JASCO 880 PU pump equipped with a Crest Pak C18T-5 ODS column and a JASCO 870 UV detector, and chromatography was run with MeOH at a flow rate of 1.0 cm^3 min^{-1}.

2.2. Synthesis of *N*-substituted 8-hydroxy-2-methyl-5-sulfamoylquinolines

Compounds **3b**–**g** were synthesized from 5-(chlorosulfonyl)-8-hydroxy-2-methylquinoline in a similar manner. Typical procedure was described for the synthesis of **3b**.

2.2.1. 8-Hydroxy-2-methyl-5-(*N*-octylsulfamoyl)quinoline (3b)

Octylamine (3.0 mL, 23 mol) was added to a solution of 5-(chlorosulfonyl)-8-hydroxy-2-methylquinoline[17] (402 mg, 1.6 mmol) in dry THF (40 mL) at room temperature, and the mixture was stirred at room temperature overnight. After the solvent had been evaporated, $CHCl_3$ (50 mL) was added to the residue. The mixture was washed with 1 M HCl (50 mL) and dried over anhydrous Na_2SO_4. The crude product was purified by column chromatography on silica gel with $CHCl_3$ to yield **3b** as a colorless solid (466 mg, 85%), mp 124–126 °C. IR (KBr): 3282, 2925, 1568, 1509, 1469, 1318, 1269, 1233, 614 cm^{-1}. ^1H NMR ($CDCl_3$) δ 0.84 (3H, t, J = 7.0 Hz), 1.09–1.37 (12H, m), 2.76 (3H, s), 2.90 (2H, q, J = 7.0 Hz), 7.15 (1H, d, J = 8.3 Hz), 7.49 (1H, d, J = 8.8 Hz), 8.16 (1H, d, J = 8.3 Hz), 8.86 (1H, d, J = 8.8 Hz). Anal. Calcd for $C_{18}H_{26}N_2O_3S{\cdot}0.3H_2O$: C, 60.75; H, 7.53; N, 7.87. Found: C, 60.79; H, 7.53; N, 8.00.

2.2.2. 5-(*N*-Decylsulfamoyl)-8-hydroxy-2-methylquinoline (3c)

Colorless solid, 38% yield, mp 124–127 °C. IR (KBr): 3289, 2921, 1563, 1504, 1471, 1326, 1281, 1207, 612 cm^{-1}. ^1H NMR ($CDCl_3$) δ 0.87 (3H, t, J = 6.7 Hz), 1.09–1.37 (16H, m), 2.76 (3H, s), 2.89 (2H, t, J = 6.7 Hz), 7.15 (1H, d, J = 8.3 Hz), 7.49 (1H, d, J = 8.8 Hz), 8.16 (1H, d, J = 8.3 Hz), 8.86 (1H, d, J = 8.8 Hz). Anal. Calcd for $C_{20}H_{30}N_2O_3S{\cdot}0.2H_2O$: C, 62.86; H, 8.02; N, 7.33. Found: C, 62.72; H, 8.23; N, 7.33.

2.2.3. 5-(*N*-Dodecylsulfamoyl)-8-hydroxy-2-methylquinoline (3d)

Colorless solid, 43% yield, mp 120–122 °C. IR (KBr): 3285, 2920, 1568, 1509, 1426, 1319, 1270, 1204, 615 cm^{-1}. ^1H NMR ($CDCl_3$) δ 0.87 (3H, t, J = 6.9 Hz), 1.09–1.37 (20H, m), 2.76 (3H, s), 2.90 (2H, t, J = 6.9 Hz), 7.15 (1H, d, J = 8.3 Hz), 7.49 (1H, d, J = 8.8 Hz), 8.15 (1H, d, J = 8.3 Hz), 8.86 (1H, d, J = 8.8 Hz). Anal. Calcd for $C_{22}H_{34}N_2O_3S$: C, 64.99; H, 8.43; N, 6.89. Found: C, 64.89; H, 8.44; N, 6.91.

2.2.4. 5-(*N,N*-Dioctylsulfamoyl)-8-hydroxy-2-methylquinoline (3e)

Colorless solid, 52% yield, mp 73–74 °C. IR (KBr): 3348, 2927, 1568, 1505, 1468, 1304, 1201, 1146, 631 cm^{-1}. ^1H NMR ($CDCl_3$) δ 0.86 (6H, t, J = 7.4 Hz), 1.12–1.45 (24H, m), 2.75 (3H, s), 3.19 (4H, t, J = 7.4 Hz), 7.13 (1H, d, J = 8.0 Hz), 7.45 (1H, d, J = 8.8 Hz), 8.10 (1H, d, J = 8.0 Hz), 8.83 (1H, d, J = 8.8 Hz). Anal. Calcd for $C_{26}H_{42}N_2O_3S{\cdot}0.1H_2O$: C, 67.23; H, 9.16; N, 6.03. Found: C, 67.14; H, 9.12; N, 5.93.

2.2.5. 5-(*N,N*-Didecylsulfamoyl)-8-hydroxy-2-methylquinoline (3f)

Colorless soild, 48% yield, mp 53–54 °C. IR (KBr): 3353, 2923, 1568, 1505, 1468, 1304, 1200, 1118, 626 cm^{-1}. ^1H NMR ($CDCl_3$) δ 0.88 (6H, t, J = 7.3 Hz), 1.12–1.43 (32H, m), 2.75 (3H, s), 3.16 (4H, t, J = 7.3 Hz), 7.13 (1H, d, J = 8.2 Hz), 7.45 (1H, d, J = 8.8 Hz), 8.10 (1H, d, J = 8.2 Hz), 8.83 (1H, d, J = 8.8 Hz). Anal. Calcd for $C_{30}H_{50}N_2O_3S{\cdot}0.1H_2O$: C, 69.21; H, 9.72; N, 5.38. Found: C, 69.08; H, 9.63; N, 5.39.

2.2.6. 5-(*N,N*-Didodecylsulfamoyl)-8-hydroxy-2-methylquinoline (3g)

Colorless solid, 43% yield, mp 45–47 °C. IR (KBr): 3285, 2920, 1568, 1509, 1426, 1319, 1270, 1204, 615 cm^{-1}. ^1H NMR ($CDCl_3$) δ 0.87 (6H, t, J = 6.9 Hz), 1.09–1.37 (40H, m), 2.76 (3H, s), 3.18 (4H, t, J = 6.9 Hz), 7.13 (1H, d, J = 8.3 Hz), 7.45 (1H, d, J = 8.8 Hz), 8.10 (1H, d, J = 8.3 Hz), 8.83 (1H, d, J = 8.8 Hz). Anal. Calcd for $C_{34}H_{58}N_2O_3S{\cdot}0.1H_2O$: C, 70.81; H, 10.17; N, 4.86. Found: C, 70.56; H, 9.97; N, 5.03.

2.3. Synthesis of vanadium complexes with quinoline ligands

Complexes **1b**–**g** were synthesized from **3b**–**g**, respectively, in a similar manner. Typical procedure was described for the synthesis of **1b**.

2.3.1. Bis[2-methyl-5-(*N*-octylsulfamoyl)-8-quinolinato]-oxovanadium(IV) (1b)

To a solution of compound **3b** (94 mg, 0.26 mmol) in CH_3CN–H_2O (1/1, 112 mL) was added $VO(acac)_2$ (35 mg, 0.13 mmol), and the mixture was refluxed overnight and then cooled to room temperature. The precipitates were collected by filtration, and washed several times with H_2O to give **1b** as a yellow solid (93 mg, 94%),

mp 204 °C (decomp). IR (KBr): 1565, 1505, 1460, 1378, 1311, 1154, 978, 788 cm^{-1}. UV–vis (c = 1 mM in DMSO): λ_{max} (ε) = 718 nm (18). Anal. Calcd for $C_{36}H_{50}N_4O_7S_2V{\cdot}0.1H_2O$: C, 56.32; H, 6.59; N, 7.30. Found: C, 56.03; H, 6.36; N, 7.36.

2.3.2. Bis[5-(*N*-decylsulfamoyl)-2-methyl-8-quinolinato]-oxovanadium(IV) (1c)

Yellow solid, 78% yield, mp 213 °C (decomp). IR (KBr): 1563, 1506, 1467, 1372, 1309, 1129, 974, 788 cm^{-1}. UV–vis (c = 1 mM in DMSO): λ_{max} (ε) = 720 nm (20). Anal. Calcd for $C_{40}H_{58}N_4O_7S_2V$: C, 58.45; H, 7.11; N, 6.82. Found: C, 58.05; H, 7.17; N, 6.67.

2.3.3. Bis[5-(*N*-dodecylsulfamoyl)-2-methyl-8-quinolinato]-oxovanadium(IV) (1d)

Yellow solid, 70% yield, mp 216 °C (decomp). IR (KBr): 1565, 1505, 1460, 1378, 1311, 1154, 978, 788 cm^{-1}. UV–vis (c = 1 mM in DMSO): λ_{max} (ε) = 718 nm (18). Anal. Calcd for $C_{44}H_{66}N_4O_7S_2V$: C, 60.18; H, 7.58; N, 6.38. Found: C, 60.05; H, 7.40; N, 6.62.

2.3.4. Bis[5-(*N*,*N*-dioctylsulfamoyl)-2-methyl-8-quinolinato]-oxovanadium(IV) (1e)

Yellow solid, 71% yield, mp 171 °C (decomp). IR (KBr): 1586, 1503, 1457, 1378, 1306, 1151, 994, 792 cm^{-1}. UV–vis (c = 1 mM in DMSO): λ_{max} (ε) = 747 nm (8). Anal. Calcd for $C_{52}H_{82}N_4O_7S_2V$: C, 63.07; H, 8.35; N, 5.66. Found: C, 62.90; H, 8.47; N, 5.63.

2.3.5. Bis[5-(*N*,*N*-didecylsulfamoyl)-2-methyl-8-quinolinato]-oxovanadium(IV) (1f)

Brown solid, 41% yield, mp 171 °C (decomp). IR (KBr): 1566, 1503, 1457, 1377, 1307, 1152, 994, 760 cm^{-1}. Anal. Calcd for $C_{60}H_{98}N_4O_7S_2V{\cdot}0.1H_2O$: C, 65.26; H, 8.96; N, 5.07. Found: C, 65.37; H, 9.27; N, 4.95.

2.3.6. Bis[5-(*N*,*N*-didodecylsulfamoyl)-2-methyl-8-quinolinato]-oxovanadium(IV) (1g)

Yellow solid, 59% yield, mp 111–113 °C. IR (KBr): 1566, 1502, 1457, 1377, 1306, 1152, 994, 792 cm^{-1}. Anal. Calcd for $C_{68}H_{114}N_4O_7S_2V$: C, 67.24; H, 9.46; N, 4.60. Found: C, 67.34; H, 9.44; N, 4.83.

2.4. Synthesis of 1-substituted 3-hydroxy-2-methyl-4(1*H*)-pyridinones

Compounds **4b–d** were synthesized from maltol in a similar manner. Typical procedure was described for the synthesis of **4b**.

2.4.1. 1-Hexyl-3-hydroxy-2-methyl-4(1*H*)-pyridinone (4b)

A mixture of maltol (4.18 g, 32.2 mmol) and hexylamine (3.42 g, 33.8 mmol) in 3% aqueous HCl solution (100 mL) was refluxed for 7 days and then cooled to room temperature. The resulting yellow solid was collected by filtration and then recrystallized from acetone to yield **4b** as a colorless solid (830 mg, 11%), mp 128–129 °C. IR (KBr): 3175, 2956, 2928, 1629, 1349, 1240, 1040, 754 cm^{-1}. ^1H NMR ($CDCl_3$) δ 0.88–0.91 (3H, m), 1.32 (6H, s), 1.68–1.72 (2H, m), 2.39 (3H, s), 3.84 (2H, t, J = 7.8 Hz), 6.38 (1H, d, J = 7.3 Hz), 7.20 (1H, d, J = 7.3 Hz). Anal. Calcd for $C_{12}H_{19}NO_2$: C, 68.87; H, 9.15; N, 6.69. Found: C, 68.77; H, 8.94; N, 6.81.

2.4.2. 1-Decyl-3-hydroxy-2-methyl-4(1*H*)-pyridinone (4c)

Colorless solid, 16% yield, mp 123–124 °C. IR (KBr): 3091, 2921, 2852, 1625, 1351, 1235, 1036, 721 cm^{-1}. ^1H NMR ($CDCl_3$) δ 0.86–0.89 (3H, m), 1.26–1.32 (14H, m), 1.70–1.73 (2H, m), 2.39 (3H, m), 3.84 (2H, t, J = 7.8 Hz), 6.37 (1H, d, J = 7.3 Hz), 7.22 (1H, d, J = 7.3 Hz). Anal. Calcd for $C_{16}H_{27}NO_2{\cdot}0.1H_2O$: C, 71.92; H, 10.26; N, 5.24. Found: C, 71.85; H, 10.27; N, 5.18.

2.4.3. 3-Hydroxy-2-methyl-1-tetradecyl-4(1*H*)-pyridinone (4d)

Colorless solid, 22% yield, mp 116–117 °C. IR (KBr): 3171, 2920, 2851, 1628, 1349, 1242, 1035, 720 cm^{-1}. ^1H NMR ($CDCl_3$) δ 0.86–0.89 (3H, m), 1.25–1.32 (22H, m), 1.72–1.73 (2H, m), 2.39 (3H, s), 3.84 (2H, t, J = 7.5 Hz), 6.37 (1H, d, J = 7.3 Hz), 7.22 (1H, d, J = 7.3 Hz). Anal. Calcd for $C_{20}H_{35}NO_2{\cdot}0.1H_2O$: C, 74.30; H, 10.97; N, 4.33. Found: C, 74.34; H, 11.10; N, 4.49.

2.5. Synthesis of vanadium coplexes with pyridinone ligands

Compounds **2b–d** were synthesized from **4b–d**, respectively, in a similar manner. Typical procedure was described for the synthesis of **2b**.

2.5.1. Bis(1,4-dihydro-1-hexyl-2-methyl-4-oxo-3-pyridinolato) oxovanadium(IV) (2b)

To a solution of **4b** (50 mg, 0.18 mmol) in H_2O (10 mL) was added dropwise $VOSO_4{-}3H_2O$ (15 mg, 0.09 mmol) in H_2O (3 mL), and the pH of the mixture was adjusted to 10 with 2 M KOH in H_2O. The resulting mixture was refluxed overnight, and then cooled to room temperature. The precipitates were collected by filtration and washed several times with H_2O to yield **2b** as a blue solid (50 mg, 95%), mp 115–116 °C. IR (KBr): 2927, 2857, 1604, 1508, 976, 718 cm^{-1}. UV–vis (c = 1 mM in DMSO): λ_{max} (ε) = 542 nm (1328). Anal. Calcd for $C_{24}H_{36}N_2O_5V{\cdot}0.1H_2O$: C, 59.18; H, 7.53; N, 5.75. Found: C, 59.15; H, 7.75; N, 5.45.

2.5.2. Bis(1-decyl-1,4-dihydro-2-methyl-4-oxo-3-pyridinolato) oxovanadium(IV) (2c)

Light blue solid, 86% yield, mp 118 °C (decomp). IR (KBr): 2924, 2853, 1604, 1547, 981, 719 cm^{-1}. UV–vis (c = 1 mM in DMSO): λ_{max} (ε) = 537 nm (847). Anal. Calcd for $C_{32}H_{52}N_2O_5V{\cdot}0.6H_2O$: C, 63.37; H, 8.84; N, 4.62. Found: C, 63.07; H, 8.95; N, 4.66.

2.5.3. Bis(1,4-dihydro-2-methyl-1-tetradecyl-4-oxo-3-pyridinolato)oxovanadium(IV) (2d)

Black solid, 59% yield, mp 127 °C (decomp). IR (KBr): 2923, 2852, 1604, 1547, 984, 719 cm^{-1}. Anal. Calcd for $C_{40}H_{68}N_2O_5V$: C, 67.86; H, 9.68; N, 3.96. Found: C, 68.00; H, 9.70; N, 4.10.

2.6. Measurement of proliferation of U937 cells

U937 cells were seeded in 12-well culture plates (0.2×10^6 cells/well) with 1485 μL/well of RPMI 1640 medium containing 5% penicillin-streptomycin and 10% fetal bovine serum (FBS). A vanadium complex synthesized as above was dissolved in dimethyl sulfoxide (DMSO) to produce a 1 mM solution, which was added to each well to produce a final concentration of 10 μM. After incubation at 37 °C under an atmosphere of 5% CO_2–95% air for 24 h, the number of viable cells was determined by staining with trypan blue.

2.7. Staining with annexin V and propidium iodide (PI)

U937 cells (0.2×10^6 cells) were suspended in 9.99 mL of RPMI 1640 medium containing 5% penicillin-streptomycin and 10% FBS, and treated with 10 μL of a 10 mM vanadyl complex in DMSO to give a final concentration of 10 μM. Cells were incubated at 37 °C under an atmosphere of 5% CO_2–95% air for 24 h, washed with cold phosphate buffered saline, collected by centrifugation, and lysed in annexin V-fluorescein (2 μL), binding buffer (100 μL), and PI (2 μL).

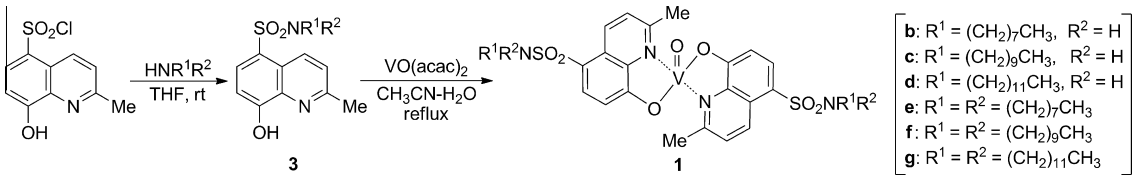

Scheme 1. Synthesis of vanadium complexes **1b–g**.

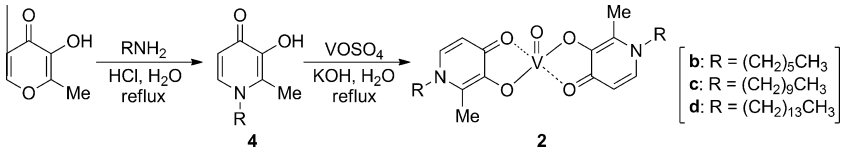

Scheme 2. Synthesis of vanadium complexes **2b–d**.

The suspension was incubated for 15 min at room temperature, and the cells were observed by fluorescence microscopy.

2.8. DNA fragmentation analysis by electrophoresis

U937 cells (0.2×10^6 cells) were suspended in 14.85 mL of RPMI 1640 medium containing 5% penicillin-streptomycin and 10% FBS. A solution of **2a–c** in DMSO was added to give a final concentration of 25 μM. Cells were incubated at 37 °C under an atmosphere of 5% CO_2–95% air for 24 h, centrifuged at 15,000 rpm for 10 min, washed with cooled phosphate buffered saline (PBS) several times, centrifuged again, and then lysed in 200 μL of lysis buffer (1 mL of 1 M Tris–HCl buffer at pH 7.4, 0.2 mL of 0.5 M EDTA, and 0.5 mL of 10% TritonX-100). Lysed cells were held at 4 °C for 10 min, and the supernatants were incubated with 2 μL of RNase A (10 mg/mL in Tris–EDTA buffer) at 50 °C for 30 min and then with 2 μL of proteinase K (10 mg/mL in distilled water) at 50 °C for 45 min. The solution was mixed with 20 μL of 5 M NaCl and 120 μL of 2-propanol, and the mixture was incubated at −20 °C for 24 h, followed by centrifugation at 15,000 rpm for 20 min. The precipitated DNA was dissolved in 5 μL of Tris–EDTA buffer and subjected to electrophoresis using a 2% agarose gel and Tris-acetate-EDTA buffer at 50 V. The DNA fragmentation pattern was visualized with a UV transilluminator.

2.9. Effect of caspase inhibitors

U937 cells (0.2×10^6 cells) were suspended in 1998 μL of RPMI 1640 medium containing 5% penicillin-streptomycin and 10% FBS, and treated with 2 μL of 100 mM caspase inhibitors in DMSO (final concentration of the inhibitor: 100 μM). After the mixture was incubated at 37 °C under an atmosphere of 5% CO_2–95% air for 1 h, 2 μL of 1 mM **2c** in DMSO was added (final concentration of **2c**: 1 μM). The mixture was incubated at 37 °C under an atmosphere of 5% CO_2–95% air for 24 h, and the number of viable cells was determined by staining with trypan blue.

3. Results and discussion

3.1. Syntheses and characterization

The reaction of 5-(chlorosulfonyl)-8-hydroxy-2-methylquinoline and amines in dry THF at room temperature yielded the quinoline ligands **3b–g** (Scheme 1). The vanadium complexes **1b–g** were obtained as precipitates by refluxing a mixture of **3b–g** and 0.5 equimolar amount of $VO(acac)_2$ in MeCN–H_2O, followed by cooling to room temperature. The pyridinone ligands **4b–d** were synthesized by the reaction of maltol with amines under acidic conditions (Scheme 2). Refluxing a mixture of **4b–d** and 0.5 equimolar amount of $VOSO_4$ in H_2O at pH 10 and then cooling to room temperature gave vanadyl complexes **2b–d** as precipitates.

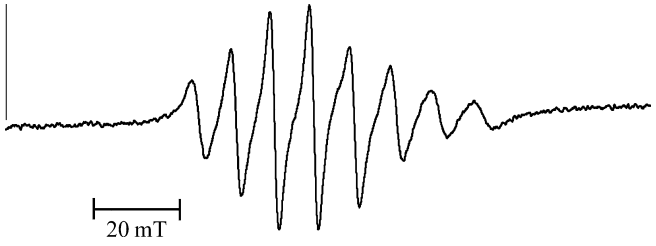

Figure 2. ESR spectrum of the complex **1b**.

As described in the Section 2, the visible absorption spectra of the vanadium complexes **1b–e** and **2b–c** in DMSO showed peaks at 718–747 nm, which can be assigned to the d–d transition of $V^{IV}O^{2+}$.[18] We further confirmed the structure of the synthesized vanadium complexes by ESR. The ESR spectra of the complexes **1b–e** and **2b–d** in THF at room temperature displayed eight-line hyperfine splitting patterns due to the unpaired electron of the ^{51}V nucleus ($I = 7/2$) (Fig. 2). This result indicated that only one mononuclear vanadium(IV) species with one unpaired electron was present in the examined sample solution. The ESR parameters g- and A-values of the complexes were calculated (Table 1). The calculated values were consistent with those of vanadyl species with the $VO(O_4)$ coordination mode reported previously.[19]

Table 1
ESR parameters of vanadyl complexes **1** and **2**

Complex	g	A (mT)
1b	1.977	9.25
1c	1.982	9.24
1d	1.978	9.18
1e	1.979	9.14
1f	1.979	8.87
1g	1.986	8.69
2b	1.973	9.68
2c	1.974	9.56
2d	1.973	9.63

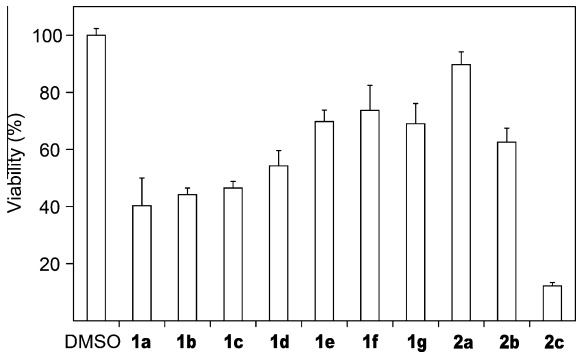

Figure 3. Viability of U937 cells (%). Dimethylsulfoxide (DMSO) was used as a control. Values are means ± SD, $n = 3$.

Table 2
IC_{50} values against U937 cells

Complex	IC_{50} (μM)[a]
2a	58.96 ± 8.85
2b	19.45 ± 3.08
2c	1.52 ± 0.37[b]
Cisplatin	15.61 ± 3.84

[a] Values are means ± SD; $n = 3$.
[b] $P < 0.05$ versus cisplatin.

Table 3
Log*P* values and molecular weights of complexes **1** and **2**

Complex	Log*P*	Molecular weight
1a	3.96	821.98
1b	3.62	765.88
1c	3.95	821.98
1d	4.38	878.09
1e	5.57	990.30
1f	6.74	1102.51
1g	8.09	1214.73
2a	2.95	427.39
2b	3.23	483.49
2c	4.16	595.71

3.2. Antiproliferative activity

Antiproliferative activities of **1a**–**g** and **2a**–**c** were evaluated by adding their DMSO solution to U937 cells in RPMI 1640 medium containing 5% penicillin-streptomycin and 10% FBS. The final concentration of the vanadium complex was 10 μM, and the mixture was incubated for 24 h at 37 °C in an atmosphere of 5% CO_2–95% air. Among the synthesized compounds, the complex **2d** showed very low solubility in DMSO, and we could not determine the activity of this compound.

The relative cell viability of the oxovanadium complexes is shown in Figure 3. The antiproliferative activities of the vanadium complexes with *N*-monoalkylated sulfamoylquinoline ligands **1b**–**d** increased in the order **1d** < **1c** < **1b**, that is, the complex with the longer alkyl chain tended to exhibit lower activity. However, the differences in activity were very small. Similarly, the *N*,*N*-dialkylated complexes **1e**–**g** showed almost equal activities, and their activities were lower than those of *N*-monoalkylated complexes **1b**–**d**. In either case, the positive effect of the alkyl chain on the activity could not be observed in the complexes with quinoline ligands. As for the complexes with pyridinone ligands, the *N*-butyl compound (**2a**) showed less potent antiproliferative activity than those with quinoline ligands. However, as we expected, the activity increased with the length of alkyl chain (**2a** < **2b** < **2c**), and the vanadium complex with the *N*-tetradecylpyridinone unit (**2c**) exhibited the highest antiproliferative activity. These results indicated that the length of the alkyl chain on pyridinone ligands was one of the important factors for determining the antiproliferative activity of vanadium complexes.

The antiproliferative activity of vanadium complexes with pyridinone ligands (**2a**–**c**) was further examined by determining the 50% inhibitory concentration (IC_{50}) values from the viability data of U937 cells. For comparison, we also measured IC_{50} value of cisplatin. As shown in Table 2, the order of IC_{50} values was **2c** < **2b** < **2a**, that is, the order of the activity was **2a** < **2b** < **2c**. The IC_{50} value of **2c** was especially noteworthy because this compound was more potent than the well-known anticancer drug cisplatin. These results clearly showed that the complex with a longer alkyl chain possessed higher antiproliferative activity.

3.3. Lipophilicity of complexes

We thought that lengthening of the alkyl chain will lead to the increase in lipophilicity of the vanadium complex with pyridinone ligands, which would result in improvement of their antiproliferative activity. In the structure–activity relationship studies of compounds with antiproliferative and/or cytotoxic activities in leukemia and tumor cells, the partition coefficients of the compounds were used as a parameter of their lipophilicity.[20–22] Recently, it was proposed that lipophilicity is an important factor to determine the insulin-mimetic activity of vanadyl complexes.[23] However, the relationships between the structure of the oxovanadium complex and its lipophilicity have not been clarified. To evaluate the lipophilicity of the vanadium complexes **1a**–**g** and **2a**–**c**, we determined the octanol/water partition coefficient (log*P*) values by the reported procedure.[16] The results are summarized in Table 3. As for the complexes with quinoline ligands (**1a**–**g**), the order of log*P* values was **1b** < **1c** ≈ **1a** < **1d** < **1e** < **1f** < **1g**. This order was the same as that of molecular weight, but different from the order of the antiproliferative activity shown in Figure 3. These results indicated that the activity of **1a**–**g** did not correlate with their lipophilicity. In contrast, the order of log*P* values of the complexes with pyridinone ligands was **2a** < **2b** < **2c**, which was the same as that of their antiproliferative activities. Indeed, as shown in Figure 4, a good correlation was obtained between the IC_{50} values and log*P* values. These results suggested that the activity of **2a**–**c** was largely affected by their hydrophobicity.

3.4. Mechanism of antiproliferative activity

We previously reported that, based on the results of annexin V-PI staining, the antiproliferative activity of **2a** can be attributed to apoptosis.[15] To confirm the apoptosis-inducing activity of **2b** and **2c**, U937 cells were treated with these complexes and then stained with annexin V and PI. Fluorescence microscopy images showed

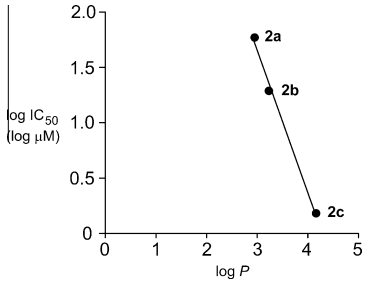

Figure 4. Relationship between log*P* values and logIC_{50} values of complexes **2a**–**c**.

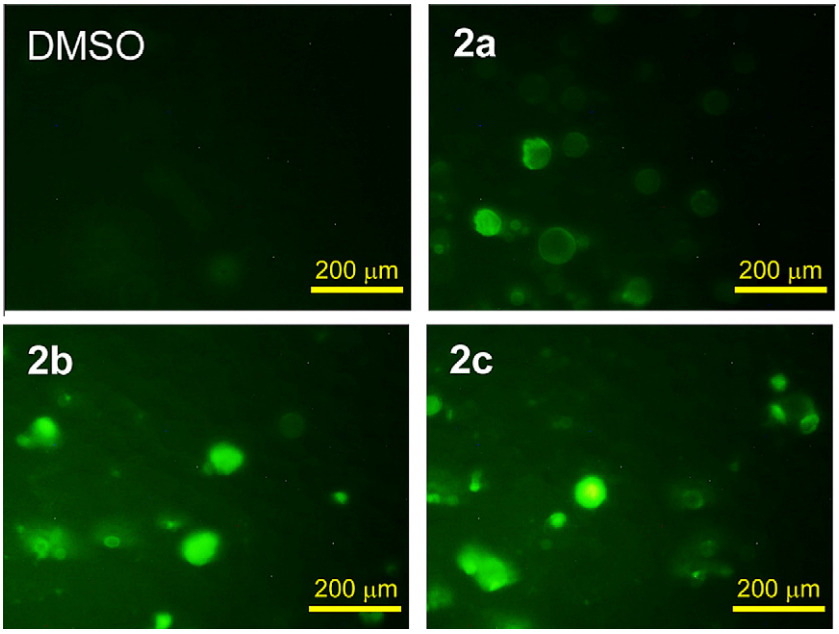

Figure 5. Fluorescence microscopy images of U937 cells treated with DMSO and **2a–c**, followed by annexin V-PI staining.

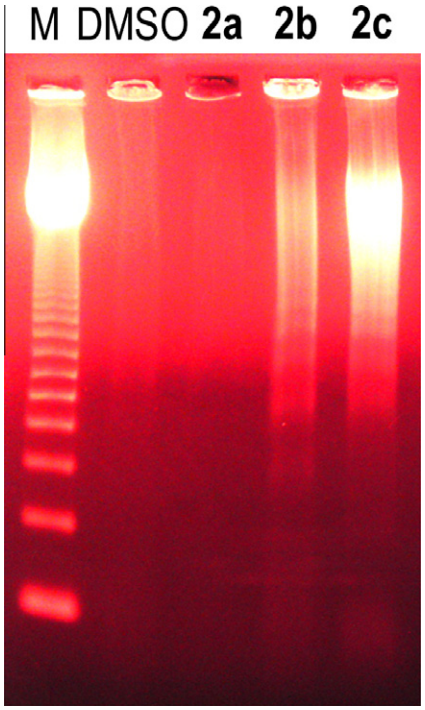

Figure 6. Agarose gel electrophoresis of DNA fragmentation induced in U937 cells by **2a–c** visualized under UV light with ethidium bromide staining (M: DNA marker).

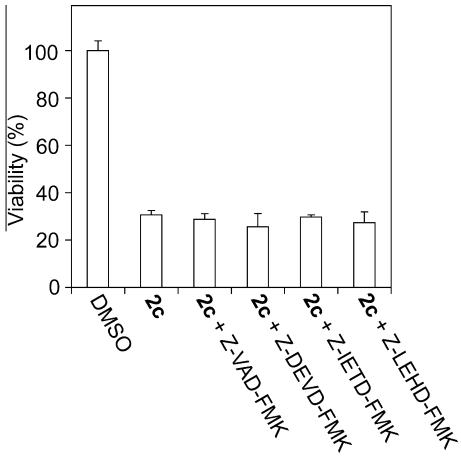

Figure 7. Viability percentages of U937 cells treated with **2c** (1 μM) and caspase inhibitors (100 μM). Values are means ± SD; $n = 3$.

only green fluorescence, suggesting that the cells were annexin V-positive and PI-negative (Fig. 5). Furthermore, typical DNA fragmentation ladders could be detected in agarose gel electrophoresis analysis of the DNA of U937 cells treated with **2b** and **2c** (Fig. 6). Therefore, the complexes **2b** and **2c** were thought to induce apoptosis in U937 cells.

Caspases play an important part in apoptosis.[24] Therefore, we next examined the participation of caspases in the apoptosis induced by **2**. We used Z-DEVD-FMK, Z-IETD-FMK, and Z-LEHD-FMK as peptide-based inhibitors of caspase-3, -8, and -9, respectively, because these caspases are involved in the main pathway of apoptosis.[25] Furthermore, Z-VAD-FMK was also used as a general caspase inhibitor. U937 cells were treated with **2c** in the presence of one of these caspase inhibitors. As shown in Figure 7, the activity of **2c** was not affected by these caspase inhibitors. These results indicated that the apoptosis of U937 cells induced by **2c** might be associated with a caspase-independent mechanism.

4. Conclusion

Oxovanadium(IV) complexes with quinoline ligands **1b–g** and pyridinone ligands **2b–d** were synthesized. The antiproliferative activity of **1a–g** toward U937 cells did not show a clear correlation with the length of alkyl chain. In contrast, a good correlation was observed between the log$P$ and logIC_{50} values of **2a–c**. Among them, **2c** showed the strongest antiproliferative activity and was more potent than cisplatin. The annexin V-PI staining experiment and agarose gel electrophoresis analysis indicated that cell death

was because of apoptosis. The activity of **2c** was not affected by the inhibitors of caspase-3, -8, and -9; therefore, the apoptosis might be associated with a caspase-independent mechanism.

Acknowledgments

The authors sincerely thank Professor Yoshio Teki (Graduate School of Science, Osaka City University, Osaka, Japan) for ESR analyses. This work was supported by a Grant from Seikei University.

References and notes

1. Desoize, B. *Anticancer Res.* **2004**, *24*, 1529.
2. Florea, A.-M.; Büsselberg, D. *Cancers* **2011**, *3*, 1351.
3. Ghosh, P.; D'Cruz, O. J.; Narla, R. K.; Uckun, F. M. *Clin. Cancer Res.* **2000**, *6*, 1536.
4. Evangelou, A. M. *Crit. Rev. Oncol. Hematol.* **2002**, *42*, 249.
5. Schieven, G. L.; Wahl, A. F.; Myrdal, S.; Grosmaire, L.; Ledbetter, J. A. *J. Biol. Chem.* **1995**, *270*, 20824.
6. Dawson, G.; Kilkus, J.; Schieven, G. L. *FEBS Lett.* **2000**, *478*, 233.
7. D'Cruz, O. J.; Dong, Y.; Uckun, F. M. *Anti-Cancer Drugs* **2000**, *11*, 849.
8. Narla, R. K.; Dong, Y.; D'Cruz, O. J.; Navara, C.; Uckun, F. M. *Clin. Cancer Res.* **2000**, *6*, 1546.
9. Narla, R. K.; Dong, Y.; Uckun, F. M. *Leukemia Lymphoma* **2001**, *41*, 625.
10. Bold, R. J.; Termuhlen, P. M.; McConkey, D. J. *Surg. Oncol.* **1997**, *6*, 133.
11. Ghobrial, I. M.; Witzig, T. E.; Adjei, A. A. *CA Cancer J. Clin.* **2005**, *55*, 178.
12. Mendoza-Ferri, M.-G.; Hartinger, C. G.; Eichinger, R. E.; Stolyarova, N.; Severin, K.; Jakupec, M. A.; Nazarov, A. A.; Keppler, B. K. *Organometallics* **2008**, *27*, 2405.
13. Dodo, K.; Minato, T.; Hashimoto, Y. *Chem. Pharm. Bull.* **2009**, *57*, 190.
14. Iitsuka, Y.; Tanaka, Y.; Hosono-Fukao, T.; Hosono, T.; Seki, T.; Ariga, T. *Oncol. Res.* **2010**, *19*, 575.
15. T. Yamaguchi, S.; Watanabe, Y.; Matsumura, Y.; Tokuoka, A.; Yokoyama, *Chem. Pharm. Bull.* In press.
16. Asami, S.; Saitoh, K. *Chem. Lett.* **2006**, *35*, 196.
17. Pearce, A.; Jotterand, N.; Carrico, I. S.; Imoeriali, B. *J. Am. Chem. Soc.* **2001**, *123*, 5160.
18. Jørgensen, C. K. *Acta Chem. Scand.* **1957**, *11*, 73.
19. Yamaguchi, M.; Wakasugi, K.; Saito, R.; Adachi, Y.; Yoshikawa, Y.; Sakurai, H.; Katoh, A. *J. Inorg. Biochem.* **2006**, *100*, 260.
20. Nakai, J.; Kawada, K.; Nagata, S.; Kuramochi, K.; Uchiro, H.; Kobayashi, S.; Ikekita, M. *Biochem. Biophys. Acta* **2002**, *1581*, 1.
21. Dodo, K.; Minato, T.; Noguchi-Yachide, T.; Suganuma, M.; Hashimoto, Y. *Bioorg. Med. Chem.* **2008**, *16*, 7975.
22. Sliva, H.; Barra, C. V.; Rocha, F. V.; Frézard, F.; Lopes, M. T. P.; Fontes, A. P. S. *J. Braz. Chem. Soc.* **2010**, *21*, 1961.
23. Adachi, Y.; Yoshida, J.; Kodera, Y.; Katoh, A.; Takada, J.; Sakurai, H. *J. Med. Chem.* **2006**, *49*, 3251.
24. Vermeulen, K.; van Bockstaele, D. R.; Berneman, Z. N. *Ann. Hematol.* **2005**, *84*, 627.
25. Fan, T.-J.; Han, L.-H.; Cong, R.-S.; Liang, J. *Acta Biochim. Biophys. Sin.* **2005**, *37*, 719.